Ferromagnetism in the metallic phase of (Ga,Mn)N nanostructures

M. A. Boselli
Instituto de Física, Universidade do Estado do Rio de Janeiro, Rua São Francisco Xavier 524, 20.500-013 Rio de Janeiro, R.J., Brazil

I. C. da Cunha Lima[a]
Instituto de Física, Universidade do Estado do Rio de Janeiro, Rua São Francisco Xavier 524, 20.500-013 Rio de Janeiro, R.J., Brazil and Instituto de Física, Universidade de São Paulo, CP 66318, 05315-970 São Paulo, SP, Brazil

J. R. Leite
Instituto de Física, Universidade de São Paulo, CP 66318, 05315-970 São Paulo, SP, Brazil

A. Troper
Centro Brasileiro de Pesquisas Físicas, Rua Xavier Sigaud, 20.500-013 Rio de Janeiro, R.J., Brazil and Instituto de Física, Universidade do Estado do Rio de Janeiro, Rua São Francisco Xavier 524, 20.500-013 Rio de Janeiro, R.J., Brazil

A. Ghazali
Groupe de Physique des Solides, UMR 7588-CNRS, Universités Paris 6 et Paris 7, Campus Universitaire Boucicaut, 140 rue de Lourmel, 75 015 Paris, France

The occurrence of ferromagnetism in the metallic phase of (Ga,Mn)N thin layers is studied by Monte Carlo simulation assuming an indirect exchange of the Ruderman–Kittel–Kasuya–Yosida type, via the spin-polarized hole system. We take into account a possible polarization of the hole gas due to the existence of an average magnetization in the magnetic layer. Transition temperatures one order of magnitude higher than in similar (Ga,Mn)As nanostructures are obtained. Two regimes are observed for the dependence of the magnetization on temperature. © *2004 American Institute of Physics.* [DOI: 10.1063/1.1646759]

GaN is a wide-gap material ideal for optical devices (light-emitting diodes detectors, and lasers) operating in the blue to the near-ultraviolet region. It is also important for electronic devices, especially in high-frequency, high-temperature and high-power transistors. GaN is usually grown in the wurtzite structure (GaN-h), although a meta-stable cubic phase can also be grown by molecular-beam epitaxy technique (GaN-c).[1] The recent observation of high transition temperatures in (Ga,Mn)N ferromagnetic phases[2] points to prospective applications in spintronics and photonics by the association of its optical, transport, and magnetic properties.

At present, a vast literature exists about the magnetic properties observed in the metallic phase of the Mn-doped III-V semiconductor (Ga,Mn)As. The ferromagnetic order in this system is understood as resulting from the indirect exchange between the Mn ions due to the local spin polarization in the hole gas.[3] The free hole concentration is a fraction (10%–20%) of the total concentration of Mn, and is provided by the Mn ions themselves, which are shallow acceptors. The magnetic order resulting from indirect exchange via spin-polarized free carriers implies a spin coherence length larger than the average distance between localized magnetic moments.

In the case of (Ga,Mn)N, there is a large discrepancy on the reported measurements concerning the transition temperature and carrier concentration. In both hexagonal and cubic phases, the hole binding energy for the Mn impurity is high, and the free gas is probably provided by other dopants. In this work, we assume that the mechanism leading to the ferromagnetic order in (Ga,Mn)N is the same as in (Ga,Mn)As, once in the metallic phase, but the sources of the free carrier gas may be different. Thus, the carrier concentration and the Mn concentration are treated as independent parameters. We obtain interesting information, however, as is shown subsequently, by studying a model structure composed by two (Ga,Mn)N layers embedded in a GaN host. We explore the interplay of the intra- and interlayer magnetic interactions as we change the separation between them, the layers thickness, and the carrier concentration. We show that, under certain circumstances, two distinct temperature ranges appear in the magnetization. We obtained transition temperatures in (Ga,Mn)N nanostructures one order of magnitude higher than in their (Ga,Mn)As analogs.

We use a Monte Carlo (MC) simulation based on an indirect exchange mechanism provided by the local interaction of the localized magnetic moments with the itinerant spin-polarized hole system. A self-consistent electronic structure calculation, which takes into account the existence of an average magnetization of the Mn ions, is used to obtain the exchange term that enters the simulation. Therefore, electronic and magnetic properties are entangled.

The interaction potential between the Fermi gas and the localized magnetic moments is well described by the Kondo-like exchange $H_{sp-d} = -I\Sigma_i \mathbf{S}_i \cdot \mathbf{s}(\mathbf{r})\,\delta(\mathbf{r}-\mathbf{R}_i)$, where the localized spin of the Mn ion $\mathbf{S}_i$ at position $\mathbf{R}_i$ will be treated as

[a]Electronic mail: ivancl@uol.com.br

a classical variable, and $\mathbf{s}(\mathbf{r})$ is the spin operator of the carrier at position $\mathbf{r}$; I is the $sp-d$ interaction. To the second-order perturbation, the correction to the energy, which is bilinear in the magnetic ion dipole moment, is

$$H_{\text{eff}} = -\sum_{i,j} (C_{ij}^{\uparrow\uparrow} + C_{ij}^{\downarrow\downarrow})S_i^z S_j^z$$
$$+ (C_{ij}^{\uparrow\downarrow} + C_{ij}^{\downarrow\uparrow})(S_i^x S_j^x + S_i^y S_j^y), \qquad (1)$$

which includes explicitly the spin-flip terms. The arrows refer to spins parallel or antiparallel to the average Mn magnetization. The exchange terms are

$$C_{ij}^{\mu\nu} = -\sum_{n\in\mu}\sum_{n'\in\nu} \phi_{n'}^*(z_i)\phi_n(z_i)\phi_n^*(z_j)\phi_{n'}(z_j)$$
$$\times \left(\frac{I}{2A}\right)^2 \chi^{n,n'}(\mathbf{R}_{ij}), \qquad (2)$$

where A is the normalization area; $\mathbf{k}$ is a wave vector in the (x,y) plane, which is parallel to the interfaces; n is the subband index; and $\phi_{n,\sigma}(z)$ is the envelope function that describes the motion of the fermion in the z direction. Notice that the summations on n and n' are restricted to those subbands with the proper spin polarization. Use has been made of the Lindhard function $\chi^{n,n'}(\mathbf{q})$ and $\chi^{n,n'}(\mathbf{R}_{ij}) = \Sigma_{\mathbf{q}} \exp[-i\mathbf{q}\cdot\mathbf{R}_{ij}]\chi^{n,n'}(\mathbf{q})$, its real-space Fourier transform.[3] The eigenfunctions $\phi_n(z_i)$ to be used in Eq. (2) are obtained by assuming the hole system to be homogeneous in the xy plane, so the Hartree term depends only on the coordinate z: $U_H(\mathbf{r}) = U_H(z)$. A uniform magnetization is also assumed in the dilute magnetic semiconductor (DMS) layers. This is made clear by Eq. (3). With the homogeneous concentration ρ of N_i magnetic impurities in the DMS layer, the $sp-d$ single-particle potential becomes

$$-I\int d^3\mathbf{R}_i \rho(\mathbf{R}_i)\mathbf{s}(\mathbf{r}).\mathbf{S}(\mathbf{R}_i)\delta(\mathbf{r}-\mathbf{R}_i)$$

$$= -N_0\beta\frac{\sigma}{2}x\langle M\rangle g(z) \equiv V_{\text{mag}}^{\text{eff}}(z), \qquad (3)$$

where $\sigma = \pm 1$ for spin parallel (upper sign) or antiparallel (lower sign) to the magnetization, $N_i/V = xN_0$ is the impurity density in terms of the Mn composition x (assumed as 5%), and N_0 is the density of the cation ions. $g(z) = 1$ if z lies inside the DMS layer, and $g(z) = 0$ otherwise. The $p-d$ exchange constant for holes β is given by $N_0\beta = -2.3$ eV.[4] Examining Eqs. (3), we see that a "magnetic barrier (well)" is introduced at the DMS layer for spins parallel (antiparallel) to the magnetization. In other words, the existence of a net magnetization $\langle M\rangle$ polarizes the hole gas by introducing an effective confining potential in our model. The eigenstates are obtained by solving the secular equation with this effective magnetic interaction, the kinetic term, and the Hartree term (due to the free carrier gas and ionized impurities). They determine the spin-polarized density of charge, the number of occupied subbands, the Fermi level, and the Fermi wave number for each occupied subband. The Hartree potential is obtained by solving the Poisson equation in the reciprocal space. After iterating up to convergence, we obtain the exchange constants in Eq. (2).

Classical spins $\mathbf{S}_i$, representing the localized magnetic moments of the Mn ions, are randomly distributed on the cation sites with concentration x. Randomness refers to both the site position and the spin orientation. They are assumed to interact through the exchange Hamiltonian defined by Eq. (1). Our calculation is self-consistent in the sense that the magnetic ion subsystem and the carrier (hole) subsystem are treated on equal footing. Concerning the electronic structure, however, we assume a homogeneous magnetization $\langle M\rangle$ at the DMS layers, which is identified with the thermal average magnetization. Disorder effects, either structural or thermal, are, in fact, included in our calculations, since the Mn ions are located randomly on cation sites in the MC simulations, and the thermal average magnetization is included through the Metropolis algorithm, which rules our MC computations. The average magnetization obtained in this way is certainly different from that one would expect from a homogeneous continuum model for spins.

A stepwise slow cooling process is accomplished, starting from a temperature larger than the transition temperature T_c, and making sure that the thermal equilibrium is reached at every temperature. Every time the net magnetization increases to reach a value of $n\times 0.1$ (n being an integer varying from 0 to 10) of the saturation, the tabulated values of the exchange interaction terms are substituted by those corresponding to the new reference $\langle M\rangle$. These ones are calculated from the hole states (eigenfunctions, eigenvalues, and Fermi wave numbers) resulting from the self-consistent calculations for this specific thermal average magnetization $\langle M\rangle$. The resulting spin configuration for the Mn ions is taken as the starting configuration for the next step at a lower temperature. The Monte Carlo procedure adopted in this way takes account of the changes in the hole gas polarization due to the presence of the established order among the localized magnetic moments in the Mn ions. The self-consistent electronic structure of the hole system and the thermal equilibrium state of the Mn magnetic moments are now coupled.

The present work is focused on the dependence of the magnetic properties of the (Ga,Mn)N on the sample parameters (e.g., sample structure geometry and carrier density) within our model of indirect magnetic interaction mediated by spin-polarized carriers. In order to compare with similar results obtained for (Ga,Mn)As, we concentrate on cubic phase samples, to avoid different behaviors coming out of differences on the host symmetry. First, a simulation is performed using two different values of the carrier density: $p = 1\times 10^{20}$ and 2×10^{20} cm^{-3}. For each one of these values, a sequence of samples is chosen, consisting of two 20 Å magnetic layers separated by a GaN spacer, whose thickness changes from $a=0$ to $a=80$ Å. The structures are supposed to lie at the center of an infinite 200 Å GaN quantum well. All samples present a paramagnetic-to-ferromagnetic transition, with transition temperatures that are almost one order of magnitude higher than those obtained by using the same model in similar (Ga,Mn)As samples. Figure 1 shows the dependence of T_c on the spacer width. This behavior of T_c is well fitted by an exponential decaying function, $y = y_0 + y_1 \exp(-x/\lambda)$, with $\lambda \approx 11$ to 12 Å, very close to the value obtained for (Ga,Mn)As: 10 Å, approximately.[3] Compared to (Ga,Mn)As, however, we observed that the peaks on the sus-
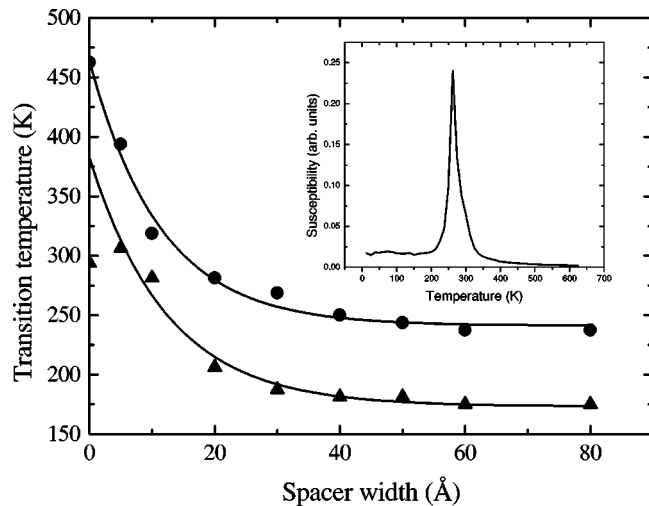
FIG. 1. Dependence of T_c on the spacer width for carrier densities $p = 1 \times 10^{20}$ cm^{-3} (triangles) and $p = 2 \times 10^{20}$ cm^{-3} (circles). Exponential fitting parameter $\lambda = 11.4$ and 12.4 Å, respectively. In the inset, the susceptibility for the low carrier density sample with a 10 Å spacer.

ceptibility (which identify T_c) are much more pronounced, as shown in the inset for $a = 10$ Å.

A precise determination of the carrier density in (Ga,Mn)N samples has not yet been established, as commented in the beginning of this letter. However, it is worthwhile to calculate how T_c changes with the free carrier concentration in a reasonable range. This is shown in Fig. 2 for a 5 Å GaN spacer. We observe that T_c increases with the carrier concentration in this range, in agreement with calculations previously reported by Dietl *et al.*[4] for (Ga,Mn)As, using a mean-field approximation. The most striking qualitative influence of the carrier concentration on the magnetization curve appears in Fig. 3, for the same samples discussed earlier. The tail we see near T_c is just a consequence of the finite sized sample in our model. However, at low carrier concentrations, we notice the appearance of two different regimes in the dependence of the magnetization on temperature. Above a certain temperature, there is a pronounced change in the slope of the magnetization curve, which remains almost constant until very close to T_c. Two straight
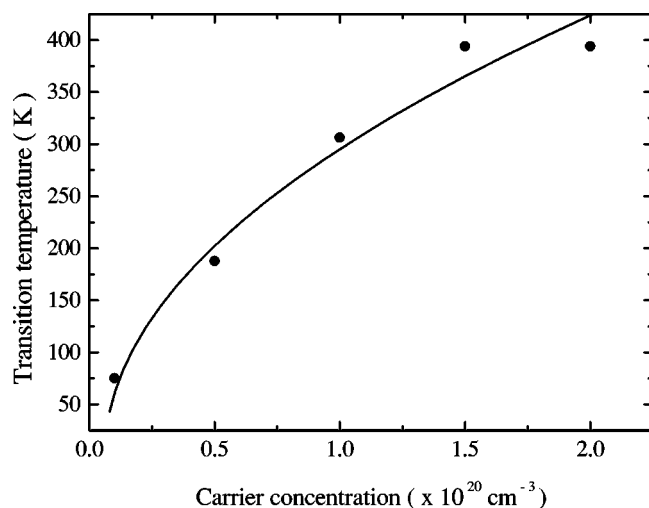

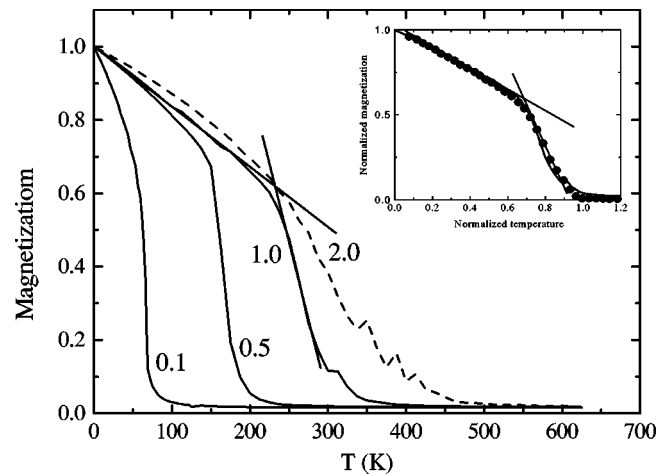FIG. 2. Dependence of T_c on the carrier concentration for a 5 Å spacer.

FIG. 3. Magnetization *versus* temperature; carrier concentrations in units of 10^{20} cm^{-3}. Inset: this calculation (solid) for a concentration of 1×10^{20} cm^{-3} and 5 Å GaN spacer, and experimental results (dots) from Ref. 5.

lines are plotted as guides to eyes representing the two temperature regimes. This behavior has already been observed experimentally by Mathieu *et al.*[5] in (Ga,Mn)As short-period superlattices. The inset shows, in normalized scales, a qualitative comparison between their measurements (dots) and our MC results (solid line) for (Ga,Mn)N bilayers. We believe this behavior is a manifestation of the interplay between inter- and intralayer interaction between the magnetic moments at the Mn sites. Acting alone, each one of these mechanisms establishes a different temperature scale. For instance, neglecting the intralayer interaction in our simulation, we obtain transition temperatures much lower than those with the two mechanisms acting together. When we take into account the real interaction, above this temperature scale, the interlayer mechanism contributing to provide a ferromagnetic alignment among the Mn spins becomes very weak. So, the magnetization in that range decreases faster with the increase of temperature. This sudden change on the magnetization slope is better observable at low carrier concentration, and for small (but finite) spacer thickness. On the other hand, in a structure consisting of a single thick layer, considered as a sequence of DMS layers with zero-width spacers, this effect on the magnetization cannot be observed, in agreement with our argument, and a smooth magnetization curve represents the magnetic order in the system.

[1] J. R. L. Fernandez, O. C. Noriega, J. A. N. T. Soares, F. Cerdeira, E. A. Meneses, J. R. Leite, D. J. As, D. Schikora, and K. Lischca, Solid State Commun. **125**, 205 (2003).

[2] S. Sonoda, S. Shimizu, T. Sasaki, Y. Yamamoto, and H. Hori, J. Cryst. Growth **237−239**, 1358 (2002); H. Hori S. Sonoda, T. Sasaki, Y. Yamamoto, S. Shimizu, K. Suga, and K. Kindo, Phys. Rev. B **324**, 142 (2002).

[3] M. A. Boselli, I. C. da Cunha Lima, and A. Ghazali, Phys. Rev. B **68**, 085319 (2003).

[4] T. Dietl, H. Ohno, and F. Matsukura, Phys. Rev. B **63**, 195205 (2001).

[5] R. Mathieu, P. Svendlindh, J. Sadowski, K. Swiatek, M. Karlsteen, J. Kanski, and L. Ilver, Appl. Phys. Lett. **81**, 3013 (2002).